Final publication available at ijr.sagepub.com

A Topological Approach to Using Cables to Separate and Manipulate Sets of Objects

Subhrajit Bhattacharya Soonkyum Kim Hordur Heidarsson
Gaurav S. Sukhatme Vijay Kumar

Abstract

In this paper we study the problem of manipulating and transporting multiple objects on the plane using a cable attached at each end to a mobile robot. This problem is motivated by the use of boats with booms in skimming operations for cleaning oil spills or removing debris on the surface of the water. The goal in this paper is to automate the task of separating the objects of interest from a collection of objects by manipulating them with cables that are actuated only at the ends, and then transporting them to specified destinations. Because the cable is flexible, the shape of the cable must be explicitly modeled in the problem. Further, the robots must cooperatively plan motions to achieve the required cable shape and gross position/orientation to separate the objects of interest and then transport them as specified. The theoretical foundation for the problem is derived from topological invariants, *homology* and *homotopy*. We first derive the necessary topological conditions for achieving the desired separation of objects. We then propose a distributed search-based planning technique for finding optimal robot trajectories for separation and transportation. We demonstrate the applicability of this method using a dynamic simulation platform with explicit models of the cable dynamics, the contact between the cable and one or more objects, and the surface drag on the cable and on the objects. We also demonstrate the working of the proposed algorithm on an experimental platform consisting of a system of two cooperating Autonomous Surface Vessels (ASVs) and stationary/anchored objects.[1]

1 Introduction

This paper addresses the motion planning for and control of the shape of a flexible cable to separate a specified set of objects from other objects and to transport the specified objects to a destination. Object manipulation is of course an important problem in robotics. Certainly conventional approaches to manipulation using robot arms with grippers has received considerable attention and is well understood [Ivan 13, Dogar 12]. In contrast, we are interested in the use of mobile robots to contact and manipulate objects without special purpose effectors. This allows more versatility but leads to many challenges. One approach relies on caging an object using multiple mobile robots. This problem has been studied for planar objects [Fink 08]. However, the ratio between the number of objects manipulated at a time, and the number of robots required for doing that is small, thus making such an approach highly inefficient for manipulating a large number of objects and for separating objects in a field with obstacles. In contrast, we propose a framework for manipulating a large number of objects with only a pair of robots.

The advantages of using ropes with robots for manipulation were demonstrated by Donald *et al* [Donald 00]. An interesting problem that arises in these settings is the modeling of the shape of the cable and the motion planning for the robots to control the position and shape of the cable. Motion planning for manipulation of rope-like flexible objects is discussed in [Saha 06]. The problem of entangling and disentangling knots and the motion planning for this problem has been addressed

[1] Parts of this work has appeared in the proceedings of the ninth Robotics: Science and Systems (RSS), 2013.

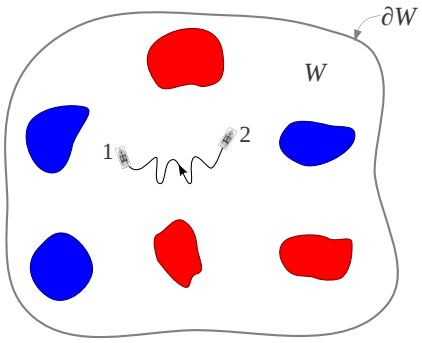

(a) The initial configuration of the cable and the two robots in the workspace W with boundary ∂W.

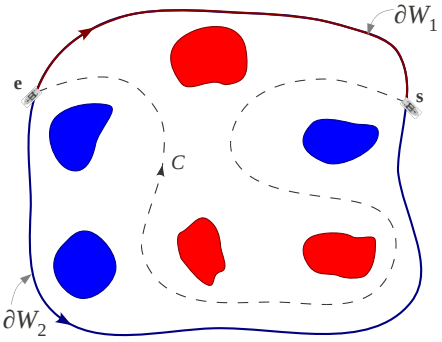

(b) A separating configuration of the cable, C, that separates the two types of objects.

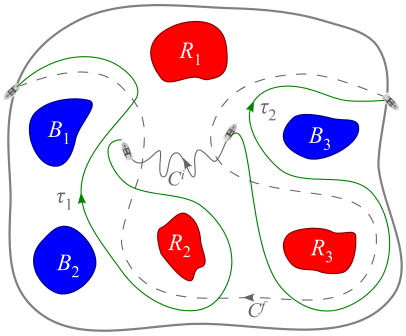

(c) A possible set of trajectories that take the cable from the initial configuration, C^i, to a configuration homotopic to the separating configuration, C^f.

Figure 1: The problem of separating the two types of objects.

in [Lamiraux 01]. Our goal, however, is the motion planning that is required to manipulate objects on the plane and we are less interested in the specific configuration of the cable. The use of robots to tow objects using cables is discussed in [Jiang 10, Cheng 09]. An extension of these ideas leads to using a cable with its ends tied to robots to cage and tow objects. Indeed this method is widely used in skimming operations on water surfaces [Robertson 10, Kerr 10]. A description of the dynamics of such systems and an analysis of the problem of cooperative skimming are provided in [Bhattacharya 11, Aranda 06]. However, this work does not explicitly address the manipulation of objects.

In this paper, we discuss the planning and control of the motions of two robots, each of which is tied to one end of a flexible cable, with the goals of (a) separating a specified set of objects from other objects; and (b) to transport the specified objects to a destination. The first step, as one might expect, is to navigate the robots around the objects so that the cable separates the objects of interest from the ones that are not of interest. The problem of finding a hypersurface separating two types of objects is studied as part of statistical classification problems [Binder 81, Suykens 99]. However such methods are susceptible to finding curves that can have disjoint components, do not have guarantees on optimality, and are statistical in nature. Moreover, the problem of finding a *separat-*

ing cable configuration (the curve) that separates the objects does not give us a necessary means of finding the trajectories of the robots that achieve that configuration. A deeper understanding of the topology of the configuration space of a system, and the use of topological techniques in problems of robot coverage and motion planning, have recently received significant attention within the robotics community [Narayanan 13, Bhattacharya 12b, Ivan 13, Tovar 08, Derenick 13, Kuderer 13] and have proven to be very effective. In this paper we discover that a topological approach to the problem under consideration is the most natural and complete. The first key contribution of this paper is a topological description of the problem of separating two sets of objects and the algebraic formulation of the separation problem. The second contribution is a complete motion planning algorithm that relies on graph search [Cormen 01] to drive the robots in order to achieve separation and then transport the objects to specified destinations. We also derive a decoupled algorithm that has the advantage of only requiring to plan in the individual robot's configuration space instead of the joint state-space.

2 Problem Description

We consider the scenario where there are two classes of objects present in a flat enclosed region, W. For convenience we will refer to the two classes as 'blue' and 'red'. Without loss of generality, one of these classes of objects will be considered to be of interest (*i.e.*, those need to be manipulated and transported), while the other consists of obstacles or objects that are not of interest. A flexible cable is attached, at its two ends, to two robots that are capable of navigating on the flat surface. Given an initial configuration of the cable and the robots (Figure 1(a)), we need to first make the robots follow trajectories to the boundary of the enclosed region, ∂W, such that the final cable configuration 'separates' the blue objects from the red, which we call the *separating configuration* (Figure 1(c)). Once that is achieved, the robots can move along ∂W to enclose one type of objects and "pull" them out, thus separating and transporting those objects.

Suppose $\mathbf{e}$ and $\mathbf{s}$ are the points on the boundary reached by the robots so that they split ∂W into ∂W_1 and ∂W_2 as in Figure 1(b). It is clear that the robot trajectories and cable configurations that describe the problem and achieve the desired objective are sufficiently described up to homotopy. That is, if C_1 and C_2 are two cable configurations that are in the same homotopy class [Bhattacharya 12b], then, *"C_1 separates the two types of objects"* $\iff$ *"C_2 separates the two types of objects"* (Figure 2(a)). Likewise, if a particular set of robot trajectories, $\{\tau_1, \tau_2\}$, carry the cable from the initial configuration to the desired separating configuration (up to homotopy), another set of trajectories, $\{\tau_1', \tau_2'\}$, that are homotopic to the first set (*i.e.* $\tau_1' \sim \tau_1$ and $\tau_2' \sim \tau_2$) will achieve the same objective.

In addition to this, it should also be noted that the homotopy class of the cable configuration that achieves the separation of the two types of objects is not unique either. For example, in Figure 2(a), the configuration C_3 is in a different homotopy class from C_1 or C_2, but still separates the two types of objects. C' in Figure 2(c) is another example. Furthermore, for a given desired separating configuration of the cable (up to homotopy), the homotopy classes of the robot trajectories that can carry the cable from its initial configuration to the separating configuration, are not unique either (Figure 2(b)). Thus, it is useful to develop a notion of optimality to more precisely define the problem objectives. It is natural to use length of the robot trajectories to the optimization criteria.

For the theoretical foundation and for setting up the optimization problem, we will make the following assumptions:

i. The objects are assumed to be stationary rigid bodies – that is, the cable cannot 'pass through' any of the objects, and that on contact of the cable with the objects the objects do not move. In

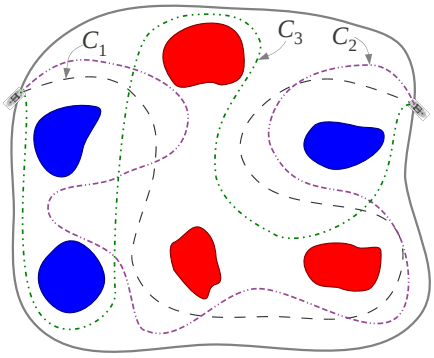

(a) Three possible cable configurations separating the two types of objects. C_1 and C_2 are homotopic. But C_3 belongs to a different homotopy class. See the curve C' in Figure 2(c) for yet another cable configuration that separates the two types of objects.

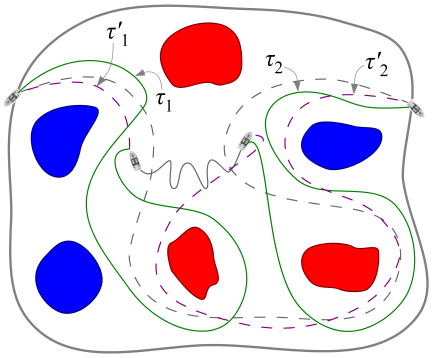

(b) The robot trajectories (up to homotopy) that can take the cable to a desired separating configuration (up to homotopy) are not unique. In this figure, τ_1 and τ'_1 are not homotopic, neither are τ_2 and τ'_2. But either of the sets of trajectories, $\{\tau_1, \tau_2\}$ or $\{\tau'_1, \tau'_2\}$, take the cable to the homotopy class shown in Figure 1(b).

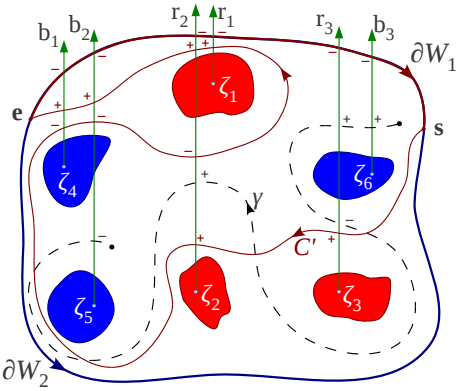

(c) ζ_i are representative points inside the objects, $R_1, R_2, \cdots, R_r, B_1, B_2, \cdots, B_b$ (in that order), and $r_i,\ i = 1, \cdots, r$ and $b_j,\ j = 1, \cdots, b$ are rays emanating from the respective points. Using the bump forms corresponding to the rays in defining the H-signature, $H(\gamma) = [0, 1, 0, 0, -1, 1]$. And, $h(\gamma) =$ "$b_3 r_2 b_2^{-1}$".

Figure 2: Homotopy and homology classes of cable configurations and trajectories.

the implementation (Section 5.3) we will however relax the conditions that the objects need to be stationary.

ii. The cable is flexible, and there is no restriction on the length of the cable (*i.e.* the cable will not fall short and tug on the robots). We assume that the cable can either be spooled out as required from a cable reel residing on the robots, or may stretch as in an elastic band.

Note that by restricting the robots' motion to a plane and assuming that they can drive over the cable, we implicitly eliminate the possibility of creating knots in the cable. In order to create a knot or a tangle a robot will need to move out of the plane, which we do not allow.

Main Contributions and Organization of the Paper

The main contribution of the paper is the use of topology-based algorithmic tools to solve the problem of separation and manipulation of sets of objects using a flexible cable carried by two robots. As descried above and illustrated in Figure 2, this problem is fundamentally topological. In Section 3 we thus start with some basic definitions related to topological descriptions of curves, and introduce some topological invariants that are fundamental to our algorithm. The main algorithmic contribution appears in Section 4, where we describe how we construct graphs that naturally incorporate the topological information such that finding a solution to the problem essentially boils down to performing an optimal search (such as A* or Dijkstra's) in the constructed graphs.

A notion of optimality is necessary in order to resolve the multiplicity of the possible solutions as illustrated above. In particular, in the joint state-space version of the algorithm described in Section 4.1 we will restrict ourselves to the optimization of sum of the lengths of the robot trajectories. This is an appropriate choice since trajectory lengths are directly related to the energy required to complete the task (*e.g.*, amount of fuel that the robots need to burn to cover the trajectories) as well as the time required to execute the trajectories. However, more complex objective functions can be used. In the decoupled and distributed planning discussed in Section 4.2, we also consider the maximum of the two trajectory lengths of the two robots as the objective that is to be minimized.

We demonstrate the practicality of the proposed algorithm in solving the real physical problem through dynamic simulations and field experiments as discussed in Section 5. For all the trajectory planning we inflate the obstacle/object map and plan the trajectories in the *inflated map* so that the planned trajectories maintain a finite separation from objects in order to avoid collision between the robots and the objects/obstacles.

3 Theoretical Foundation

Let W be a 2-dimensional simply connected and bounded region. Suppose it contains a set of objects, $\mathcal{O} = R_1 \cup R_2 \cup \cdots \cup R_r \cup B_1 \cup B_2 \cup \cdots \cup B_b \subseteq W$, where $R_1, R_2, \cdots, R_r$ are r counts of red objects, and $B_1, B_2, \cdots, B_b$ are b counts of blue objects. Each object, R_i or B_j, is assumed to be connected. Thus, throughout this paper we will denote the "free" space (the configuration space) of the individual point robots as $X := (W - \mathcal{O})$ (we will use both notations interchangibly).

3.1 Curves in a Topological Space

Both cable configurations and robot trajectories are 1-dimensional curves in $(W - \mathcal{O})$. They can thus be defined as continuous maps from the interval $[0, 1]$ to $(W - \mathcal{O})$.

In a topological space X, a curve, $\gamma : [0, 1] \to X$, is called *closed* if $\gamma(0) = \gamma(1)$. A curve, γ, is called *embedded* [Munkres 99] if $\gamma(t) \neq \gamma(t'), \forall t \neq t'$ (*i.e.* the curve does not intersect

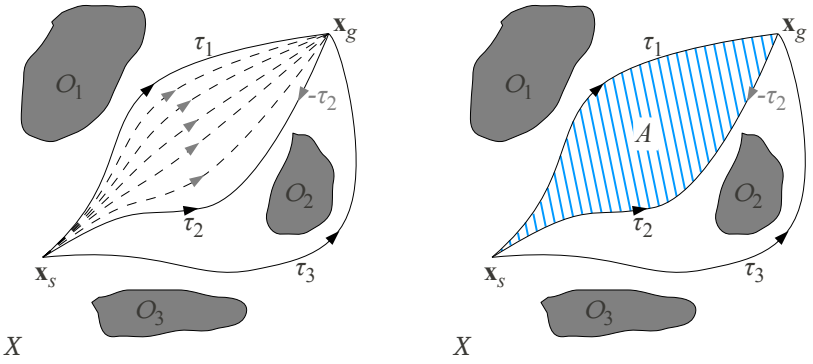

(a) τ_1 is homotopic to τ_2 since there is a continious sequence of trajectories representing deformation of one into the other. τ_3 belongs to a different homotopy class since it cannot be continuously deformed into any of the other two.

(b) τ_1 is homologous to τ_2 since there exists an area A (shaded region) such that $\tau_1 \sqcup -\tau_2$ is the boundary of A. τ_3 belongs to a different homology class since such an area does not exist between τ_3 and any of the other two trajectories.

Figure 3: Illustration of homotopy and homology equivalences. In this example τ_1 and τ_2 are both homotopic as well as homologous.

itself). [In our problem we will only require that the separating cable configuration be embedded (Proposition 1), but other curves need *not* be embedded.]

Given a curve, $f : [0,1] \to X$, we define the following curves:

i. For $0 \le \alpha < \beta \le 1$, $f|_{[\alpha,\beta]} : \begin{array}{l}[0,1] \to X \\ t \mapsto f((\beta-\alpha)t+\alpha)\end{array}$.

That is, $f|_{[\alpha,\beta]}$ is the part of the curve lying between the parameter values of α and β.

ii. $-f : \begin{array}{l}[0,1] \to X \\ t \mapsto f(1-t)\end{array}$. That is, $-f$ is the same curve as f, but with opposite orientation.

iii. for another curve $g : [0,1] \to X$ with $f(1) = g(0)$,

$$f \sqcup g : \begin{array}{l}[0,1] \to X, \\ t \mapsto \begin{cases} f(2t), \text{ if } t < 1/2 \\ g(2t-1), \text{ if } t \ge 1/2 \end{cases}\end{array}.$$

That is, $f \sqcup g$ is the curve obtained by 'joining' the end of f with the start of g.

The line integral of a differential 1-form, $\omega = u\mathrm{d}x + v\mathrm{d}y$, over a curve γ is defined as $\int_\gamma \omega := \int_0^1 (u\dot{\gamma}_x + v\dot{\gamma}_y)\,\mathrm{d}t$.

3.2 Homology and Homotopy Invariants

Definition 1 (Homology classes of curves) *In a topological space X, two curves $\gamma_1, \gamma_2 : [0,1] \to X$ connecting the same start and end points, are called homologous (or belong to the same homology class) iff γ_1 together with γ_2 (the latter with opposite orientation) forms the complete boundary of a (oriented) 2-dimensional subset embedded in X (see Figure 3).*

Formally, in the notation of [Hatcher 01], γ_1 and γ_2 are homologous iff $\gamma_1 \sqcup -\gamma_2$ belongs to the trivial class of the first homology group of X, denoted by $H_1(X)$. That is, $[\gamma_1 \sqcup -\gamma_2] = \mathbf{0} \in H_1(X)$

[Bhattacharya 12b, Hatcher 01].

A *homology invariant* is a function, H, from the space of all curves in $(W - \mathcal{O})$ (with fixed end points) to another much smaller space (in this case, a vector space), such that $H(\gamma_1) = H(\gamma_2)$ iff γ_1 is homologous to γ_2.

In [Bhattacharya 12b] we proposed a homology class invariant (called the H-signature) that is based on simple results from complex analysis. However, the possible choice of such invariants has been broadened in [Bhattacharya 13], where the choice of the vector of differential 1-forms, which needs to be integrated over γ to obtain the invariant, has been proven to be any complete set of generators of the *de Rham cohomology group*, $H^1_{dR}(W - \mathcal{O})$. In particular, the *bump* 1-*forms* [Bott 82], $\omega_j = -\upsilon(y - \zeta_{j,y})\delta(x - \zeta_{j,x})\mathrm{d}x$, (where δ is the *Dirac delta function*, and its integral, υ, is the *heaviside step function* – that is, informally speaking, ω_j are analogous to a *Dirac delta* distribution over rays emanating from *representative points* ζ_j along positive Y axis) is a choice that has the simple interpretation of counting the number of times the curve, γ, *intersects* the ray emanating from ζ_j (see Figure 2(c)). In particular, define, $\#_j\gamma := \int_\gamma \omega_j =$ (Number of times γ crosses the ray emanating from ζ_j from left to right) $-$ (Number of times γ crosses the ray emanating from ζ_j from right to left). Then, $H(\gamma) = [\#_1\gamma, \#_2\gamma, \cdots, \#_n\gamma]^T$. For closed loops the value of H-signature won't depend (up to a scalar multiple) on the choice of the differential 1-forms, as long as they form a generating set of the first *de Rham cohomology group*, $H^1_{dR}(W - \mathcal{O})$ [Bott 82], and the elements in the vector will compute the *winding numbers* about ζ_j. Let $H(\gamma)$ be the H-signature of any curve, $\gamma : [0, 1] \to (W - \mathcal{O})$, with respect to the objects $R_1, R_2, \cdots, R_r, B_1, B_2, \cdots, B_b$ (in that order).

In this paper, however, we will require the concept of *homotopy* more often, which is described next. We use a lower-case 'h' for homotopy (as in h-signature or h-augmented graph as described later), as opposed to an upper-case 'H' for homology.

Definition 2 (Homotopy classes of curves) *In a topological space, X, two curves $\gamma_1, \gamma_2 : [0, 1] \to X$ connecting the same start and end points, are homotopic (or belong to the same* homotopy class*) iff one can be continuously deformed into the other without intersecting any obstacle – refer to Figure 1(a) of [Bhattacharya 12b].*

Formally, if $\gamma_1 : [0, 1] \to X$ and $\gamma_2 : [0, 1] \to X$ represent the two trajectories (with $\gamma_1(0) = \gamma_2(0) = \mathbf{x}_s$ and $\gamma_1(1) = \gamma_2(1) = \mathbf{x}_g$), then γ_1 is homotopic to γ_2 iff there exists a continuous map $\eta : [0, 1] \times [0, 1] \to X$ such that $\eta(\alpha, 0) = \gamma_1(\alpha)\ \forall\alpha \in [0, 1]$, $\eta(\beta, 1) = \gamma_2(\beta)\ \forall\beta \in [0, 1]$, and $\eta(0, \gamma) = \mathbf{x}_s, \eta(1, \mu) = \mathbf{x}_s\ \forall\mu \in [0, 1]$ [Bhattacharya 12b, Hatcher 01]. Alternatively, in the notation of [Hatcher 01], γ_1 and γ_2 are homotopic iff the closed curve $\gamma_1 \sqcup -\gamma_2$ belongs to the trivial class of the first homotopy group of X, denoted by $\pi_1(X)$. That is, $[\gamma_1 \sqcup -\gamma_2] = \mathbf{0} \in \pi_1(X)$.

As described in [Bhattacharya 12b], two curves being homotopic implies that they be homologus as well. But the converse is not necessarily true.

Homotopy invariants, in general, are much more difficult to design and compute. *Homotopy groups*, unlike *homology groups*, do not have the natural structure of a vector space [Hatcher 01]. However, for curves in 2-dimensional plane with punctures (*i.e.* obstacles/objects) as in $(W - \mathcal{O})$, there are some relatively simple representations of the homotopy group and a way of computing the homotopy class of a given curve. In literature [Grigoriev 98, Hershberger 91, Tovar 08, Hatcher 01, Bhattacharya 12a, Narayanan 13] several similar, but different representations have been proposed — all concerning construction of "words" as homotopy class invariants. As discussed in Appendix B, the equivalence of these representations can be shown. We choose a representation that tradition-

ally appear in topology literature [Hatcher 01] and is one of the simplest ones as far as the required construction is concerned. This homotopy invariant is described as follows:

We consider *representative points*, ζ_i as before, and *non-intersecting* rays (we choose them to be parallel), $r_1, r_2, \cdots, r_r$ and $b_1, b_2, \cdots, b_b$, emanating from the red and blue objects respectively (Figure 2(c)). We form a *word* by tracing γ, and consecutively placing the letters of the rays that it crosses, with a superscript of '$+1$' (assumed implicitly) if the crossing is from right to left, and '-1' if the crossing is from left to right. Thus, for example, the word for γ in Figure 2(c) will be "$b_3 r_3 r_3^{-1} r_2 b_2^{-1}$". We can *reduce* this word by canceling the same letters that appear consecutively but with opposite superscript signs. Thus, the word for γ in Figure 2(c) can be reduced to "$b_3 r_2 b_2^{-1}$". This reduced word representation is a *homotopy invariant* for open curves (with fixed end points), γ, and we will write this as $h(\gamma)$ and call it the "h-signature of γ". However, it is important to note that we cannot exchange position for arbitrary pairs of letters in the word (*i.e.* the juxtaposition of letters is *non-commutative*). Unlike the *homology invariant*, this is not a vector, but an element of the *non-abelian* group *freely generated* [Scott 64, Hatcher 01] by $\{r_1, r_2, \cdots, r_r, b_1, b_2, \cdots, b_b\}$. Thus, although *words* can't be added in the sense of vectors, they can be concatenated under the non-commutative *group operation*, '$\star$'. Also, the inverse of a word, $\mathfrak{w}$, written as $\mathfrak{w}^{-1}$, is the h-signature of the same curve but with opposite orientation (*i.e.* $h(-\gamma) = (h(\gamma))^{-1}$), and is a word where the order of the letters are reversed, and the exponent of each letter is flipped (so that $\mathfrak{w} \star \mathfrak{w}^{-1} =$" ", the identity element). Thus, $(\mathfrak{w}_1 \star \mathfrak{w}_2)^{-1} = {\mathfrak{w}_2}^{-1} \star {\mathfrak{w}_1}^{-1}$. As an example, ("$b_3 r_2 b_2^{-1}$")$^{-1}$ ="$b_2 r_2^{-1} b_3^{-1}$".

However, if the curve is a closed loop (*e.g.* $(C' \sqcup \partial W_1)$ in Figure 2(c)), there is no preferred starting point from where we should start tracing the curve and write the word. Thus, for such curves we need to consider the *cyclic permutations* of the letters in the reduced words to be equivalent. That is, a word, "$abcde$" will be considered to be the same as "$cdeab$". Thus, when reducing a word, we need to consider the cyclic permutations, and thus cancel a letter at the beginning of the word that appears at the end as well, but with opposite superscript signs. For example, in Figure 2(c), if we trace the curve, $C' \sqcup \partial W_1$, starting at the point $\mathbf{e}$, we get,

$h(\partial W_1 \sqcup C') = h(\partial W_1) \star h(C')$
= "$b_1^{-1} b_2^{-1} r_2^{-1} r_1^{-1} r_3^{-1} b_3^{-1}$" $\star$ "$r_3 r_2 b_1^{-1} b_2^{-1} r_2^{-1} r_1 r_2 b_2 b_1$"
= "$b_1^{-1} b_2^{-1} r_2^{-1} r_1^{-1} r_3^{-1} b_3^{-1}\ r_3 r_2 b_1^{-1} b_2^{-1} r_2^{-1} r_1 r_2 b_2 b_1$"
= "$r_3^{-1} b_3^{-1}\ r_3 r_2 b_1^{-1} b_2^{-1} r_2^{-1}$"
(after canceling the letters at the start & the end),

which is the completely reduced word.

The *homotopy invariant* of a curve, γ, is the *reduced word* constructed in the described way, with cyclic permutations of a word being considered equivalent when γ is closed. In Appendix B we present a more technical discussion, only short of a formal proof, on the justification behind such words being homotopy invariants of curves.

In Section 4 we will describe how we incorporate this homotopy information inside an h-augmented graph and use an optimal graph search algorithm (such as A*) in it to find optimal trajectories in different homotopy classes in order of their path costs, without knowing the *words* for the classes to start with.

It is easy to note that for closed curves, the value of the *homology invariant* described earlier as integral over the bump 1-forms, does not depend on the choice of the direction of the rays emanating from ζ_i. But the *homotopy invariant* word is highly dependent on the choice of the direction of the rays.

The Hurewicz map: The characteristic distinction between *homotopy* and *homology* is that

the first homotopy group, generally being non-abelian (non-commutative), yields a classification with a finer resolution, while the homology group, being always an abelian (commutative) group, yields a coarser classification of trajectories. Thus, while trajectories that are homotopic are also homologous, the converse is not necessarily true (see Fig. 1 of [Bhattacharya 12b]).

The Hurewicz map [Hatcher 01] can be used to compute the *homology* invariant from a given *homotopy* invariant of a closed curve. We write h_* to denote this map from the space of h-signatures (words) to the space of H-signatures (vectors), and it is essentially the *abelianization* map.

Thus, to compute the H-signature from a given h-signature, we simply let the letters in the word commute. Thus, from the earlier example of Figure 2(c), we had $h(\partial W_1 \sqcup C')$ = "$r_3^{-1}b_3^{-1}r_3r_2b_1^{-1}b_2^{-1}r_2^{-1}$". Letting the letters commute we have the word "$r_1^0r_2^0r_3^0b_1^{-1}b_2^{-1}b_3^{-1}$" (with 0 superscript indicating that the letter is absent). Since the 6 components of the H-signature vector correspond to the objects R_1, R_2, R_3, B_1, B_2 and B_3 respectively, we thus have $H(\partial W_1 \sqcup C') = \mathsf{h}_*(\text{"}r_3^{-1}b_3^{-1}\ r_3r_2b_1^{-1}b_2^{-1}r_2^{-1}\text{"}) = [0,0,0,-1,-1,-1]^T$.

3.3 Propositions on Object Separation & Cable Manipulation

Proposition 1 *Suppose C is an embedded cable configuration such that $C(0), C(1) \in \partial W$ (*i.e. *the cable ends lie on the boundary of the environment). Say the end points of C splits ∂W into two parts: ∂W_1 and ∂W_2 (which themselves are curves in $(W - \mathcal{O})$). We assign orientation to ∂W_1 and ∂W_2 such that $C \sqcup \partial W_1$ and $C \sqcup \partial W_2$ are closed loops (Figure 1(b)). Then, C separates the two types of objects (*i.e.*, it is a* separating configuration*) iff one of the following holds for the vector $H(C \sqcup \partial W_1)$:*

i. The first r components are all 1 or all -1, and the last b components are all 0.

ii. The last b components are all 1 or all -1, and the first r components are all 0.

Note that from the definition of H-signature, $H(C \sqcup \partial W_1) = H(C) + H(\partial W_1)$. Also, in these conditions the choice of ∂W_1 over ∂W_2 is made without loss of generality. The conditions could have been stated in terms of ∂W_2 as well.

Sketch of Proof. The proof follows from the very definition of homology (see Figure 2(a)). First we note that $C \sqcup \partial W_1$ is a Jordan curve [Gamelin 01] inside W (since C is embedded). Hence there is a simply-connected region in W (not considering the objects) enclosed by $C \sqcup \partial W_1$. The objects (and their representative points) that this region will contain will manifest as a ± 1 in the corresponding components of the vector $H(C \sqcup \partial W_1)$. Since $C \sqcup \partial W_1$ is Jordan, it will wind around each of the enclosed points in the same direction (all clockwise or all anti-clockwise), thus making the corresponding components of the vectors either all $+1$ or all -1. All the other components will be 0. The statement of the proposition simply states that the enclosed representative points will be ones corresponding to the red objects or the blue objects, while the ones not enclosed will be ones corresponding to objects of the other color. ■

At this point it is instructive to illustrate why, in the above proposition, we used the homology invariant instead of homotopy invariant. Consider the curve C' in Figure 2(c), which clearly separates the red objects from blue. However we previously saw that the *reduced word* for $(C' \sqcup \partial W_1)$ is, $h(C') \star h(\partial W_1)$ = "$r_3^{-1}b_3^{-1}\ r_3r_2b_1^{-1}b_2^{-1}r_2^{-1}$". Likewise the *reduced word* $h(C') \star h(\partial W_2)$ = "$r_3r_2b_1^{-1}b_2^{-1}r_2^{-1}r_1r_2b_2b_1$". Neither of these words are helpful in identifying the fact that C' separates the blue objects from the red. However, $H(C') + H(\partial W_1) = [0,0,0,-1,-1,-1]^T$, and $H(C') + H(\partial W_2) = [1,1,1,0,0,0]^T$ – both satisfying the condition of Proposition 1 (note that the first 3 components of the vector correspond to R_1, R_2 & R_3, while the last 3 correspond to B_1, B_2 & B_3), thus indicating that C' indeed separates the blue from the red objects.

Proposition 2 *(Refer to Figure 1(c)) Let C be a starting cable configuration (which has an orientation from robot '2' to robot 1', as shown in Figure 1(a)) and C' be a final cable configuration (which may or may not be a separating configuration). Then the trajectories τ_1 and τ_2 for the two robots carry the cable from initial configuration to the separating configuration (up to homotopy) if and only if the closed loop $(C \sqcup \tau_1 \sqcup -C' \sqcup -\tau_2)$ is* null homotopic *[Hatcher 01],* i.e. $h(C \sqcup \tau_1 \sqcup -C' \sqcup -\tau_2) = h(C)\star h(\tau_1)\star h(C')^{-1}\star h(\tau_2)^{-1} =$ *" ", is the empty word (*identity element*).*

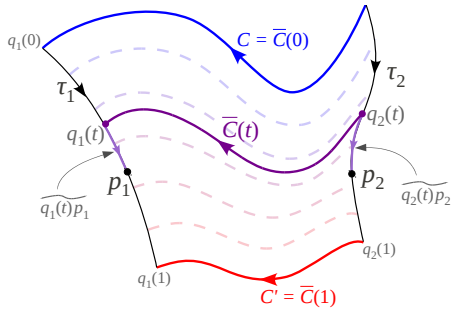

Figure 4: Illustration for Proof of Proposition 2.

Sketch of Proof. We note that unlike in Proposition 1 we don't have the luxury of assuming that $(C \sqcup \tau_1 \sqcup -C' \sqcup -\tau_2)$ will be Jordan (see, for example, Figure 1(c)). First, suppose trajectories τ_1 and τ_2 carries the cable from configuration C to final configuration C'. We choose two arbitrary points, p_1 and p_2, on the trajectories τ_1 and τ_2 respectively, as shown in Figure 4. Next consider the sequence of cable configurations from C to C' as the robots carry it. We can thus construct a continuous function (a homotopy), $\overline{C} : [0,1] \times [0,1] \to (W - \mathcal{O})$, such that $\overline{C}(0,\cdot) \equiv C(\cdot)$ and $\overline{C}(1,\cdot) \equiv C'(\cdot)$, and $\overline{C}(t)$ is a general intermediate cable configuration. Such a curve, $\overline{C}(t)$, has its end points $q_1(t) \in \tau_1$ and $q_2(t) \in \tau_2$ (Figure 4). We consider the curve connecting $q_1(t)$ to p_1 and lying on τ_1 (call it $\widetilde{q_1(t)p_1}$), and the one connecting $q_2(t)$ to p_2 and lying on τ_2 (call it $\widetilde{q_2(t)p_2}$). Thus, the sequence of curves, $D(t) := \left(-\widetilde{(q_2(t)p_2)} \sqcup \overline{C}(t) \sqcup \widetilde{(q_1(t)p_1)}\right)$, defines a homotopy between curves connecting p_1 and p_2. Thus, $D(0) \sqcup -D(1)$ is null-homotopic. That is, $\left(-\widetilde{(q_2(0)p_2)} \sqcup \overline{C}(0) \sqcup \widetilde{(q_1(0)p_1)}\right) \bigsqcup - \left(-\widetilde{(q_2(1)p_2)} \sqcup \overline{C}(1) \sqcup \widetilde{(q_1(1)p_1)}\right) \equiv (C \sqcup \tau_1 \sqcup -C' \sqcup -\tau_2)$, is null-homotopic.

Conversely, if $(C \sqcup \tau_1 \sqcup -C' \sqcup -\tau_2)$ is null-homotopic, one can construct a homotopy, D, as before, and hence construct a sequence of curves $\overline{C}$, that takes the cable from C to C'. ■

4 Implementation

For simplicity, we assume that the environment, W, is a rectangular region, and all the rays, $r_j,\ j = 1, 2, \cdots, r$ and $b_j,\ j = 1, 2, \cdots, b$, are parallel, pointing along the positive Y axis. Furthermore, we restrict the final goals of the robots to the left and right boundaries of the environment (∂W_l at $x = x_l$ and ∂W_r at $x = x_r$ respectively), but they need to reach the opposite edges. Thus, a part of the boundary, ∂W_2, will never intersect any of the rays (Figure 5(a)), and hence $H(\partial W_2) =$

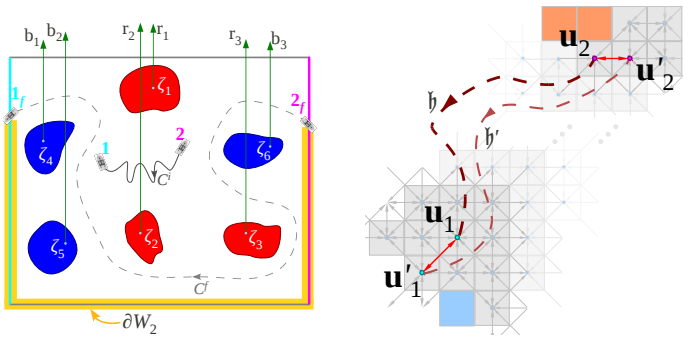

(a) The rectangular environment with the goal of the robots being the left (cyan line) and right (magenta line) boundaries. ∂W_2 does not intersect any of the rays (all of which point in the positive Y direction).

(b) Robots 1 and 2 navigating on copies of graph, $\mathcal{G}$, formed by uniform discretization of configuration space. Change in the h-signature of the cable due to transitions within the graph is also illustrated.

Figure 5: The environment and its discretization.

$[0, 0, \cdots, 0]^T$ and $h(\partial W_2) =$ "". This simplifies the computation of $H(C^f \sqcup \partial W_2)$ for Proposition 1 to the computation of $H(C^f)$.

We use a discrete representation of the environment, and construct a graph, $\mathcal{G}$, by placing a vertex in every discrete cell and by establishing an edge between the vertices of adjacent cells. From such a graph we can construct an H-augmented graph, $\mathcal{G}_H$ (for keeping track of the homology invariants), or an h-augmented graph, $\mathcal{G}_h$ (for keeping track of the homotopy invariants), as described in [Bhattacharya 12b].

While the graph, $\mathcal{G}$, itself can be quite arbitrary, for simplicity we used a uniform 8-connected discrete representation (see Figure 5(b)) of the environment for all our simulations and experiments.

4.1 Planning in Joint State-space

The problem under consideration is to plan optimal trajectories that would take a given initial cable configuration, C^i, to a separating cable configuration, and the robot 1 reaches the left (or right) edge of W, while robot 2 reaches the right (or left) edge. In this section we describe an algorithm that searches for the optimal solutions in the joint state-space of the two robots and the homotopy class of the cable. A graph, $\mathcal{J} = \mathcal{G} \times \mathcal{G}$, is defined as the *graph Cartesian product* of two copies of $\mathcal{G}$. Thus, for every pair of vertices, $\mathbf{u}_1, \mathbf{u}_2 \in V(\mathcal{G})$, a vertex in $V(\mathcal{J})$ is of the form $(\mathbf{u}_1, \mathbf{u}_2)$, and for every pair of edges of the form $[\mathbf{u}_1 \rightsquigarrow \mathbf{u}'_1], [\mathbf{u}_2 \rightsquigarrow \mathbf{u}'_2] \in E(\mathcal{G})$ ('$\rightsquigarrow$' indicating the direction of an edge), there exists an edge $[(\mathbf{u}_1, \mathbf{u}_2) \rightsquigarrow (\mathbf{u}'_1, \mathbf{u}'_2)] \in E(\mathcal{J})$. We are given an initial vertex in the joint state-space, $(\mathbf{u}^i_1, \mathbf{u}^i_2)$ — the initial positions of the robots, and an initial configuration of the cable (up to homotopy) in form of the h-signature of the cable, $\mathfrak{h}_i$ (which, as defined earlier, is a *reduced word*).

In order to incorporate the information about the homotopy class of the cable in the search problem, we define an augmented graph, $\mathcal{J}_h$, such that a vertex in this graph contains the additional information of the h-signature of the cable that is being carried by the robots. This, in essence, is similar to the H-augmented graph construction detailed in [Bhattacharya 12b]. The explicit construction

is as follows: The initial vertex in $\mathcal{J}_h$ is $\mathbf{v}_i = (\mathbf{u}_1^i, \mathbf{u}_2^i, \mathfrak{h}^i)$, which contain the information about the initial positions of the robots and the h-signature of the initial cable configuration, $\mathfrak{h}^i = h(C^i)$. A transition of the robots from $(\mathbf{u}_1, \mathbf{u}_2, \mathfrak{h})$ to $(\mathbf{u}_1', \mathbf{u}_2', \mathfrak{h}')$ will mean (due to Proposition 2) that the h-signature of the resultant cable configuration is equal to $\mathfrak{h}' = h(-\tau_2)\star\mathfrak{h}\star h(\tau_1)$ (recall, '$\star$' is concatenation, followed by reduction), where τ_1 and τ_2 are trajectories taken by the robots for the transition (see Figure 5(b)). Thus, for each edge of the form $[(\mathbf{u}_1, \mathbf{u}_2) \rightsquigarrow (\mathbf{u}_1', \mathbf{u}_2')] \in E(\mathcal{J})$, emanating from $[(\mathbf{u}_1, \mathbf{u}_2)] \in V(\mathcal{J})$, the vertex $(\mathbf{u}_1, \mathbf{u}_2, \mathfrak{h}) \in V(\mathcal{J}_h)$ is connected to neighbors $(\mathbf{u}_1', \mathbf{u}_2', h(\overrightarrow{\mathbf{u}_2'\mathbf{u}_2})\star\mathfrak{h}\star h(\overrightarrow{\mathbf{u}_1\mathbf{u}_1'})) \in V(\mathcal{J}_h)$ (where, $[\mathbf{a} \rightsquigarrow \mathbf{b}]$ is used to indicate an edge in edge set, $E(\mathcal{G})$, from vertex $\mathbf{a}$ to $\mathbf{b}$, and $\overrightarrow{\mathbf{ab}}$ is the curve/line segment that constitutes the edge. $\overrightarrow{\mathbf{ba}}$ is the same curve but with opposite orientation). This gives us the recipe to construct $\mathcal{J}_h$ incrementally starting at $(\mathbf{u}_1^i, \mathbf{u}_2^i, \mathfrak{h}^i)$.

We choose the optimization objective to be the sum of the lengths of the robot trajectories since trajectory lengths are directly related to the energy required to complete the task as well as the time required to execute the trajectories. Thus, the cost of the edge $[(\mathbf{u}_1, \mathbf{u}_2, \mathfrak{h}) \rightsquigarrow (\mathbf{u}_1', \mathbf{u}_2', \mathfrak{h}\star h(\overrightarrow{\mathbf{u}_1\mathbf{u}_1'})\star h(\overrightarrow{\mathbf{u}_2'\mathbf{u}_2}))] \in E(\mathcal{J}_h)$ is chosen to be the sum of the lengths of the edges $[\mathbf{u}_1 \rightsquigarrow \mathbf{u}_1']$ and $[\mathbf{u}_2 \rightsquigarrow \mathbf{u}_2']$ in $E(\mathcal{G})$. For this cost and with the left and right boundaries as goal, an *admissible heuristic function* is $f(\mathbf{u}_1, \mathbf{u}_2, \mathfrak{h}) = \min\left((u_{1,x} - x_l) + (x_r - u_{2,x}), (u_{2,x} - x_l) + (x_r - u_{1,x})\right)$, which is a lower bound on the cost to reach a goal from $(\mathbf{u}_1, \mathbf{u}_2, \mathfrak{h})$ (where, $u_{j,x}$ is the X coordinate of a vertex $\mathbf{u}_j$ and $u_{j,y}$ is its Y coordinate).

Starting at the initial vertex, $(\mathbf{u}_1^i, \mathbf{u}_2^i, \mathfrak{h}^i)$, we thus keep *expanding* the vertices in the graph, $\mathcal{J}_h$, using a search algorithm (we use Dijkstra's [Dijkstra 59] or A* [Hart 68] since they are complete, optimal and deterministic) until we reach a goal vertex. A vertex $(\mathbf{u}_1, \mathbf{u}_2, \mathfrak{h})$ is deemed as goal if $\mathbf{u}_1 \in \partial W_l$ and $\mathbf{u}_2 \in \partial W_r$ (or vice-versa), and if $\mathsf{h}_*(\mathfrak{h}) + H(\partial W_2)$ $(= \mathsf{h}_*(\mathfrak{h}))$ satisfies the condition of Proposition 1 (*i.e.*, it is a separating cable configuration).

Planning in the joint state-space gives the flexibility of easily incorporating additional constraints (such as inter-robot collision avoidance, communication constraints, etc.) as well as using more complex cost functions.

4.2 Decoupled Planning: A Distributed Approach

While the approach of planning in joint state-space is complete and optimal, it suffers from the obvious drawback of being slow and inefficient since the graph, $\mathcal{J}$, is very large and is of high degree, being a discrete representation of a 4-dimensional space. However, it is possible to decouple the searches for the two robots in two copies of $\mathcal{G}_h$ (the h-augmented graph of $\mathcal{G}$, described next), each of which are discrete representation of two-dimensional spaces, and run those searches parallely (in parallel threads in our C++ implementation). Consequently, collecting the solutions obtained from each parallel process as they progress, and checking if they together give a valid solution for attaining a separating configuration, we are able to conclude when the optimal solution is found, and thus halt the threads to conclude the search process.

The h-augmented graph, $\mathcal{G}_h$, is very similar to the concept of the H-signature augmented graph, $\mathcal{G}_H$ described in [Bhattacharya 12b], only with the homology invariants being replaced by the homotopy invariants. Corresponding to a given $\mathbf{u} \in V(\mathcal{G})$, there exists a discrete set of the augmented states, $(\mathbf{u}, \mathfrak{h}) \in V(\mathcal{G}_h)$, for each homotopy class of trajectories (with h-signature $\mathfrak{h}$) from an initial vertex, $\mathbf{u}^i$, to the vertex $\mathbf{u}$. Clearly $(\mathbf{u}_j^i, \text{“ ”}) \in V(\mathcal{G}_h)$ is the start vertex corresponding to the trajectory of zero length. Edges emanating from $(\mathbf{u}, \mathfrak{h})$ are thus of the form $[(\mathbf{u}, \mathfrak{h}) \rightsquigarrow (\mathbf{u}', \mathfrak{h} + h(\overrightarrow{\mathbf{u}\mathbf{u}'}))] \in E(\mathcal{G}_h)$, corresponding to every $[\mathbf{u} \rightsquigarrow \mathbf{u}'] \in E(\mathcal{G})$. The cost of such

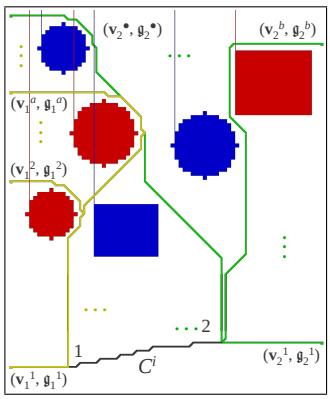

(a) Optimal paths in different homotopy classes corresponding to goal vertices $(\mathbf{v}_j^1, \mathfrak{g}_j^1), (\mathbf{v}_j^2, \mathfrak{g}_j^2), \cdots \in \mathcal{G}_{h,j}$ are found in parallel threads for robot $j = 1$ (yellow) and robot $j = 2$ (green).

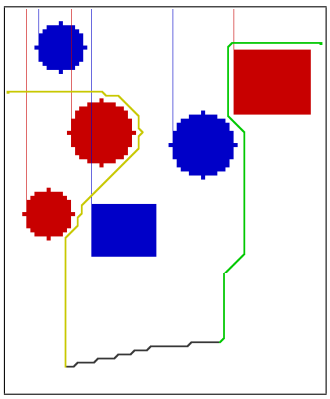

(b) A compatible combination of paths (with end vertices $(\mathbf{v}_1^a, \mathfrak{g}_1^a)$ and $(\mathbf{v}_2^b, \mathfrak{g}_2^b)$) is such that the end points, $\mathbf{v}_1^a$ & $\mathbf{v}_2^a$, lie on the opposite edges of W, and $\mathsf{h}_*((\mathfrak{g}_2^b)^{-1} \star h(C^i) \star \mathfrak{g}_1^a)$ satisfies the condition of Proposition 1.

Figure 6: Decoupled and distributed planning: Optimal paths with different h-signatures found for the two robots in parallel threads, and costs of compatible pairs are compared to find the optimal compatible pair.

an edge is chosen to be the Euclidean length of $\overrightarrow{\mathbf{uu}'}$. An *admissible heuristic function* for this choice of cost, and with goal as $\partial W_l \cup \partial W_r$, is $f(\mathbf{u}, \mathfrak{h}) = \min(u_x - x_l, x_r - u_x)$.

Thus, we start with two copies of the augmented graph, $\mathcal{G}_{h,1}$ and $\mathcal{G}_{h,2}$, in two parallel threads (that branch off from a main thread), for robots 1 and 2. In robot j's copy of the graph, we start expanding the vertices from (*i.e.*, initiate the *open list* with) the vertex $(\mathbf{u}_j^i, \text{“ ”}) \in \mathcal{G}_{h,j},\ j = 1, 2$. We keep expanding the vertices in the respective graphs, and keep storing a path every time ∂W_l or ∂W_r is reached via a new homotopy class for the robot (*i.e.* if $(\mathbf{v}, \mathfrak{g})$ is expanded, with $\mathbf{v} \in \partial W_l \cup \partial W_r$, then the vertex is bookmarked as a potential desired goal for robot j if the homotopy class $\mathfrak{g}$ is not same for any of the previously bookmarked vertices for the robot). It is important to note that for each of the robots such optimal paths with different h-signatures are found in the order of their costs since we use an optimal search algorithm (Dikjstra's/A* [Hart 68]).

Suppose for robot 'j' such potential goal vertices are $\{(\mathbf{v}_j^1, \mathfrak{g}_j^1), (\mathbf{v}_j^2, \mathfrak{g}_j^2), (\mathbf{v}_j^3, \mathfrak{g}_j^3), \cdots\}$ with costs of the respective optimal paths $c_j^1 \leq c_j^2 \leq c_j^3 \leq \cdots$, for $j = 1, 2$ (Figure 6(a)). In order to find the optimal combination of paths, we define a *partial order* [Stanley 00], $\preccurlyeq$, on $\mathbb{R}^2$, to compare the cost of pairs of paths, (c_1^m, c_2^n). One obvious choice is to compare the sum of the path costs: $(c_1^m, c_2^n) \preccurlyeq (c_1^\mu, c_2^\nu) \iff c_1^m + c_2^n \leq c_1^\mu + c_2^\nu$. However, the issue with this choice is that a lower joint cost may be highly asymmetric, while one would desire that the task of carrying the cable is evenly distributed among the two robots, and not one of the robots end up traveling most of the distance while the other travels very little. For this, we choose to minimize the maximum of the costs of the two trajectories instead of their sum. Thus, we define the partial order to be

$$(c_1^m, c_2^n) \preccurlyeq (c_1^\mu, c_2^\nu) \iff \text{Either } \max(c_1^m, c_2^n) < \max(c_1^\mu, c_2^\nu), \text{ or,}$$
$$\big(\max(c_1^m, c_2^n) = \max(c_1^\mu, c_2^\nu) \text{ and } \min(c_1^m, c_2^n) \leq \min(c_1^\mu, c_2^\nu)\big)$$

which we call the *sorted lexicographic order*.

Thus, as the main thread of the program receives the two sequences of optimal paths to the left/right boundaries with different h-signatures from the two different threads, it keeps checking them in pairs. A pair of potential goal vertices, $(\mathbf{v}_1^m, \mathfrak{g}_1^m)$ and $(\mathbf{v}_2^n, \mathfrak{g}_2^n)$, is deemed '*compatible*' (Figure 6(b)) if the corresponding final cable configuration is a separating configuration. Now, recall that due to Proposition 2, the h-signature of the final cable configuration is equal to $(\mathfrak{g}_2^n)^{-1} \star h(C^i) \star \mathfrak{g}_1^m$. Thus, for this to be a *separating configuration*, due to Proposition 1, the required condition is that $\mathsf{h}_*((\mathfrak{g}_2^n)^{-1} \star h(C^i) \star \mathfrak{g}_1^m) + H(\partial W_2)$ be a vector with first r components ± 1 and rest zeros, or last b components ± 1 and rest zeros. We keep record of the most optimal of such *compatible* pairs (*i.e.*, the one with *lowest* (c_1^a, c_2^b), where comparisons are made using '$\preccurlyeq$').

Say at an instant the most optimal pair has cost (c_1^*, c_2^*). Since the optimal paths with different h-signatures are found in order of their costs, if robot j finds a path such that its cost is greater than current value of $\max(c_1^*, c_2^*)$ (or, if we were using the sum of the pairs in defining the partial order, then $c_1^* + c_2^*$), we can say for sure that none of the paths to be discovered for robot j after that point can be part of a more optimal pair. Hence we stop the search for robot j. When the searches for both the robots end, it can be concluded that the current optimal pair is the global optimal one. We also do check for and eliminate robot trajectories that loop around objects either by checking explicit self-intersection or checking whether the h-signature contains the same letter consecutively more than once. A similar check is also done on the h-signature of the final cable configuration to prevent wrapping around objects.

As a side-note, we would like to point out that a distributed implementation over multiple threads, as proposed in this section, can be used in more generic setups. Multiple problems coupled by constraints can be decoupled and solved in parallel threads, while performing cross-validation for constraint satisfaction in a central main thread, until a solution satisfying the coupling constraints is found. An interested reader may look into [Samar 07, Bhattacharya 10] for similar approaches.

Some Notes on Complexity

The complexity of the graph searches involved is the usual for an uniform degree graph: $O(V_e \log(V_e))$, where V_e is the number of vertices *expanded* during the search. It is to be noted that we do not construct the graph $\mathcal{G}_h$ from before, and that graph itself is infinite because of the infinitely many possible homotopy classes. However, in our search algorithm we *generate* the vertices and edges of the graphs on the fly, starting at the start vertices. The number of vertices that need to be generated or expanded before a separating configuration is found will depend largely on the configuration of the red and blue objects, and is difficult to estimate for the most general setup. However, in particular, there may be simple configurations of the objects such that the very first pair of robot trajectories (obtained from the parallel threads in the decoupled planning approach) may be a separating configuration. However, the worst case complexity will in fact be exponential in the number of objects present in the environment because of the combinatorial nature of the homotopy classes in the environment.

5 Results

We implemented the planning in the joint state-space as well as the decoupled planning in C++ programming language with ROS integration, and used A* algorithm to search in the respective h-augmented graphs. All computations were performed on a system with dual-core processor with clock speed 2.6 MHz and 4 Gb memory. Throughout this paper we consider an uniform discretiza-

tion of the environment for simplicity. However, the techniques developed in this paper is not restricted to any specific discretization scheme or even a specific search algorithm. A more detailed discussion on the generality of the technique can be found in [Bhattacharya 12b].

5.1 Joint State-space Plan

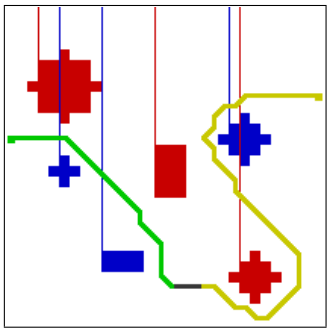

(a) Planning in the joint state-space took 4250s. The sum of the costs of two trajectories is 65.598 discretization units.

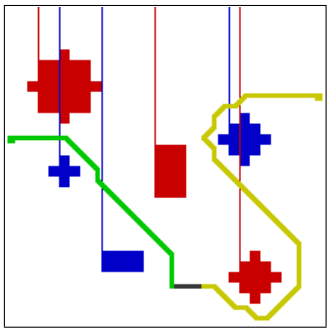

(b) The distributed decoupled planning gives result with the same optimal cost, but takes about $2s$ to run.

Figure 7: A simple 30×30 environment with $r = b = 3$. The green & yellow are the trajectories of the robots. The rays emanating from ζ_j are also shown. The dark gray segment indicates the initial cable configuration.

The search in the discrete representation of the 4-dimensional joint state-space, $\mathcal{J}_h$, is prohibitively expensive for large environments. Figure 7(a) shows the result in a simple environment, 30×30 discretized, and with 3 objects of each type. The search took about 4250 s and expanded 1484999 vertices in $\mathcal{J}_h$. Figure 7(b) shows the result obtained for same problem, but using the decoupled planning (and using sum of the cost of the trajectories for defining the partial order, $\preccurlyeq$, for being consistent). The result has the same optimal cost as the joint state-space planning, but took less than 1 s with 19144 and 19593 vertices being expanded in $\mathcal{G}_{h,1}$ and $\mathcal{G}_{h,2}$. All the objects were *inflated* to avoid collision.

5.2 Decoupled Planning

In this section we present results obtained using the decoupled, distributed implementation. The sorted lexicographic order was used for the partial order, '$\preccurlyeq$'. Figure 8(a) show the plans obtained for two robots in a 100×100 discretized environment. The planning took about 1.3 s, and expanded 39764 and 40066 vertices in the graphs of the two robots. Figure 8(b) shows the result in a much larger (400×400 discretized) environment. The planning time for this case was 490 s, with 1086182 and 1079670 vertices being expanded.

Finally, we present a result along with a simple dynamic simulation created using the open-source 2-D physics engine, *Box2D* [Catto 11], illustrating the process of separating the two types of objects. The environment in Figure 9(a) is 150×200 discretized. The blue objects are static obstacles, and the red ones are the ones that need to be separated and transported. The ends of the cables were modeled as point robots and controlled using a simple PD controller to follow the planned

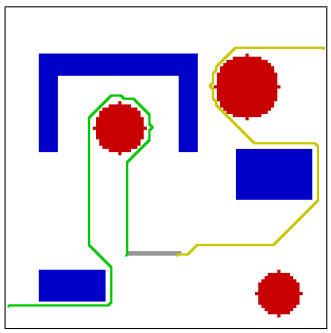

(a) The planned trajectories in a 100 × 100 discretized environment.

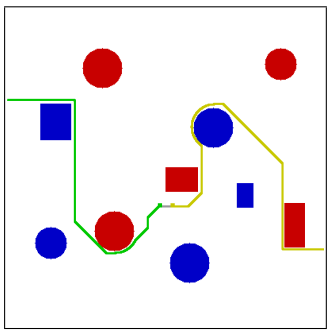

(b) The planned trajectories in a 400 × 400 discretized environment.

Figure 8: Decoupled, distributed plans. Initial cable is shown in gray/black. Optimal planned trajectories are in green and yellow.

trajectories. The red objects were given very high inertia so that their drifts are minimal when the robots are navigating to attain the separating configuration and the cable touches the objects. Figures 9(b)-(f) shows snapshots from the dynamic simulation (also see Extension 1). It is only near the end of attaining the separating configuration that enough *pull* is applied by the roots to transport the objects.

5.3 Fast Re-planning

So far we have planned the trajectories with the assumptions that the object remain stationary as the robots follow the planned trajectories. This is a fair practice even when the objects move or drift moderately from their original positions — the homotopy classes remain indifferent to small perturbations in the positions of the objects. This, in the first place, was one of the advantages behind using a topological approach — topology is robust and invariant to small perturbations in the metric information.

However, a re-planning is necessary when the objects move significantly such that that the topological classes of the planned trajectories change (*e.g.*, an object drifts and crosses the remaining planned robot trajectory or the rays emanating from the representative points of two objects cross each other). Such motions are possible due to the interactions between the cable and the objects when the objects are free to move. Instead of solving the entire problem every time the environment changes by small amounts, we invoke a re-planning algorithm only when two objects exchange the order of the X coordinates of their representative points (*i.e.*, the *rays* emanating from ζ_j cross each other) or one of the planned trajectories become invalid (due to an object moving on top of it).

Suppose $\mathfrak{g}_1$ and $\mathfrak{g}_2$ are the h-signatures for the trajectories lying ahead of the robots (*i.e.* the part yet to be traversed) just before one of the triggers for re-planning happens. We set $\mathfrak{g}'_j = \mathfrak{g}_j,\ j = 1, 2$. If the trigger was caused due to switching of the X coordinates of two representative points, we interchange the positions of the corresponding letters in the words $\mathfrak{g}'_1$ and $\mathfrak{g}'_2$ wherever they appear side-by-side. We thus re-plan trajectories for the robots in $\mathcal{G}_{h,j},\ j = 1, 2$ (starting at vertex $(\mathbf{p}_j, \text{“ ”})$, where $\mathbf{p}_j \in \mathcal{G}$ is the current vertex position of robot j) and with the constraints that the new trajectories need to have h-signature of $\mathfrak{g}'_j$.

Since for these re-plannings we know the desired h-signatures, it is possible to construct a more

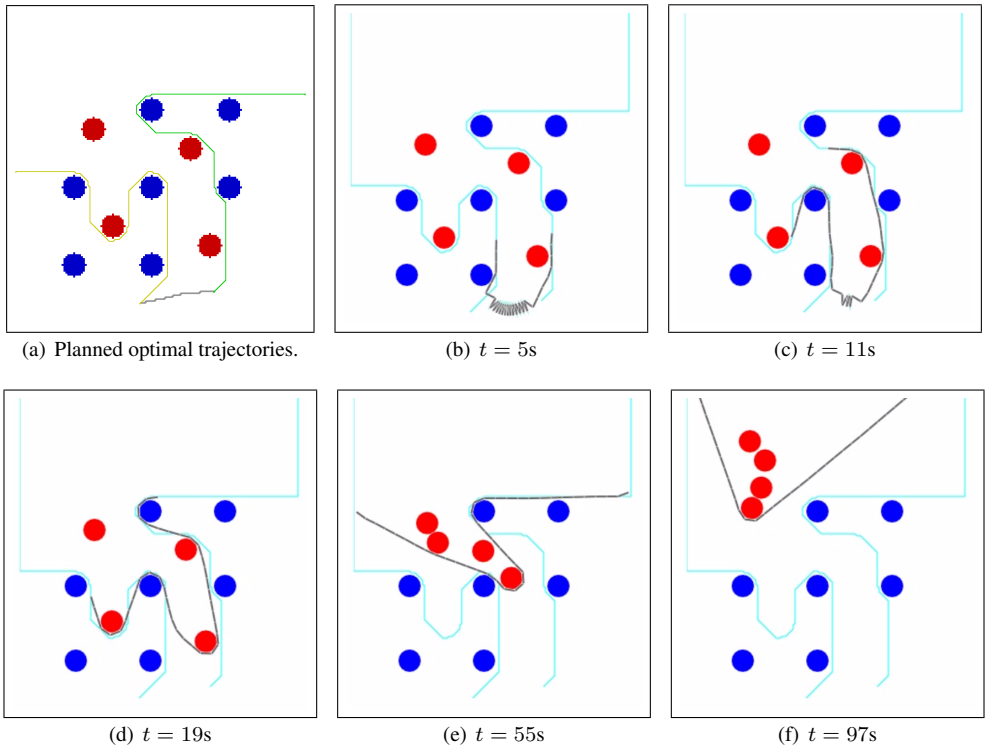

(a) Planned optimal trajectories. (b) $t = 5$s (c) $t = 11$s

(d) $t = 19$s (e) $t = 55$s (f) $t = 97$s

Figure 9: Separation and transportation of objects in presence of obstacles (also see Extension 1). (a): The environment with obstacles (blue) and objects (red) to be transported. (b)-(f): Dynamic simulation illustrating the process of separation and transportation. Grey curve is the cable, while the planned trajectories are shown in cyan.

efficient, yet admissible, heuristic function than before for performing the new searches using A* algorithm: Consider the vertex $(\mathbf{u}, \mathfrak{h})$ in the h-augmented graph used for the re-planning for robot 'j'. The h-signature of the path to a goal vertex from that vertex is thus $\mathfrak{h}^{-1} \star \mathfrak{g}'_j$. Suppose the representative points corresponding to the letters appearing in $\mathfrak{h}^{-1} \star \mathfrak{g}'_j$ are $\zeta_{\sigma_1}, \zeta_{\sigma_2}, \cdots, \zeta_{\sigma_m}$. It is obvious that the remaining part of a valid trajectory after $(\mathbf{u}, \mathfrak{h})$ will have to cross each of the rays emanating from these ζ_{σ_k} in this order (besides possibly crossing others that will cancel out). This allows us to design the following heuristic function as a lower bound of the cost (*i.e.*, admissible) for reaching a goal state:

$$f\left((\mathbf{u}, \mathfrak{h})\right) = \sum_{i=1}^{m-1} |\zeta_{\sigma_{i+1},x} - \zeta_{\sigma_i,x}| \;+\; |\zeta_{\sigma_m,x} - x_g| \;+\; \begin{cases} f_8(\mathbf{u}, \zeta_{\sigma_1}), \text{ if } u_y < \zeta_{\sigma_1,y}, \\ |u_x - \zeta_{\sigma_1,x}|, \text{otherwise} \end{cases}$$

where $f_8(\mathbf{u}, \mathbf{v}) = \sqrt{2}\min(|u_x - v_x|, |u_y - v_y|) + \big||u_x - v_x| - |u_y - v_y|\big|$ is an admissible heuristic for a 8-connected graph.

Such re-planning of trajectories will be able to take into account arbitrary motions of the objects, including collision between the objects, as long as a valid separating configuration exists. It is possible that a separating configuration ceases to exist due to objects of different colors drifting and

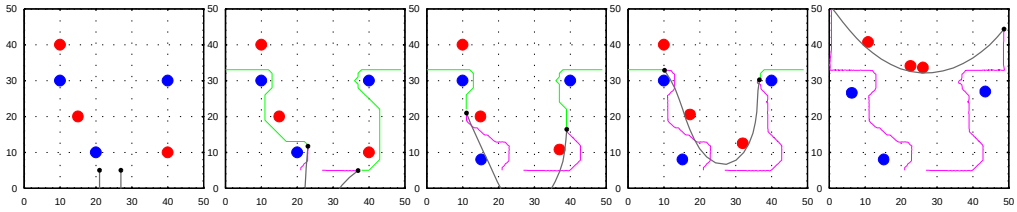

(a) $t = 0.00$ s (b) $t = 58.06$ s (c) $t = 178.35$ s (d) $t = 298.65$ s (e) $t = 479.10$ s

Figure 10: Dynamic simulation with fast re-planning for separation of objects. The gray curve is the cable, with black dots marking robots at its ends. Green curves are the planned trajectories. Magenta curves are the robot footprints. Red & blue disks are the rigid freely-floating objects. Also see Extension 1.

ending up touching each other, and hence re-planning would not find a solution. This situation is however unlikely and would be prevented in the first place due to the re-planning being triggered when one of the objects cross a robot trajectory. However if such a case indeed arises, we reduce the size of the different-colored touching objects (or the safety padding around them) in performing the re-plan, so that the subsequent interactions between the freely-floating objects and the cable/robots *opens up* a solution. We demonstrate the practicality of this approach in solving the physical problem of separating the objects through a dynamic simulation as described next.

Dynamic Simulation with Re-planning

For the purpose of testing the re-planning algorithm, we built an accurate real-time dynamic simulation platform for the cable (modeled as a serial chain) and freely floating disk-shaped objects on a fluid. Using Lagrangian mechanics we developed the equations of motion with realistic modeling of drag forces [Bhattacharya 11], and modeled the contacts using linear complementarity conditions [Kim 13]. We used a simple feedback (PD) controller to make each robot follow the paths generated by the planner as described in [Kim 13].

Figure 10 (and Extension 1) shows the dynamic simulation result on a simple environment with 3 red and 3 blue objects. All the objects are identical in size and inertia, and can move freely. Figure 10(a) shows the initial configuration of the system. As the objects move and the environment changes significantly, the planned paths of the robot are re-computed (shown by green curves in Figures 10(b)-(e)). The final figure illustrates that we were able to successfully separate the red objects from the blue ones.

5.4 Experimental Results

The field experiments were conducted in Puddingstone Lake, San Dimas, CA. Two identical Autonomous Surface Vessels (ASVs) were used, each around 2 m long and 0.8 m wide, capable of speeds up to 1.6 m/s, using two electric thrusters and a rudder for control. Both were equipped with a GPS, an IMU with integrated compass and an onboard computer for control. Six buoys (the objects to be separated) were placed in the water, anchored fairly tightly with weights to the bottom to prevent movement, in an area 25 m $\times$ 35 m, and their locations recorded manually using GPS. The displacements of the buoys from their original positions were minimal during the experiment, moving moderately only when they are tugged upon by the rope. The anchoring was necessary because

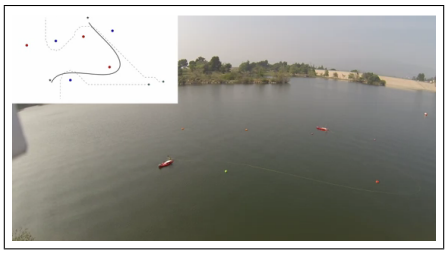

Figure 11: Experimental setup showing the ASVs.

without it the buoys would have drifted very fast due to current and wind and would be stranded on shore before the experiment could be started. For the experiments we assume that the objects remain stationary, and hence the objective of the experiment is to plan and attain a separating configuration for the cable without transporting the objects. An un-actuated cable spool was mounted on each of the ASVs and spooled on them was a floating rope, connected between the ASVs. This was done to reduce the drag that the water exerts on the rope during movement and also to be able to provide sufficient length of rope during the experiment. When the ASVs moved, the drag exerted on the rope caused more rope to pull of the spools causing the ASVs to effectively lay down the rope in their paths. In order to show the change in position of the objects as the cable tugged on them, post-processed live positions of the buoys over the course of the experiment were extracted from the overhead camera data. Figure 11 shows the experimental setup.

To record the experiment, particularly the position and shape of the rope, a camera, in an adjustable tilt mount, was mounted on top of a 9 m mast which stood on shore close to the experiment area, overlooking it. The ASVs were moved to a starting position and the planner was run based on the configuration of the targets and ASVs. The resulting plan was then executed on the ASVs.

The camera data processing was done as follows: First, the rope shape and buoy positions were manually extracted from one frame per second. Since the positions were extracted from uncalibrated images, they were then undistorted using parameters from a previous camera calibration that had been performed using a checkerboard. A perspective projection was computed from the initial positions of the buoys and applied to the images to get a get a top-down view of the rope line with a known scale.

During the experiment, the ASV on the right hand side of the formation was commanded a path of 62 m while the one on the left was commanded a path of 41 m. The length of the actual traveled paths were 86 m for the ASV on the right and 46 m for the ASV on the left. The underactuated ASVs (with limited propeller motor power) were unable to compensate for the drag on the floating rope and thus were not able to follow the commanded paths exactly. However the executed paths were homotopic to the commanded ones and the correct separation was achieved. The experiment was halted (the separated set of buoys not dragged away) once the ASVs reached their end positions due the buoys being anchored.

The accompanying video (Extension 1) shows one run of the experiment from the view of the mast-mounted camera. The animation in the top left corner (as well as the screenshots in Figure 12) shows the processed top-down view of the experiment with the assigned colors of the targets, planned path and ASV, buoy and rope movements during the experiment.

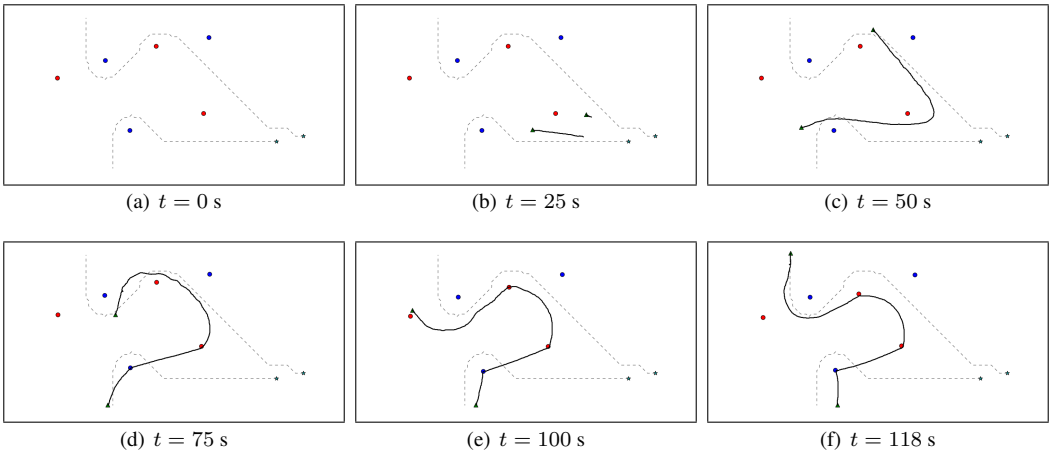

(a) $t = 0$ s (b) $t = 25$ s (c) $t = 50$ s

(d) $t = 75$ s (e) $t = 100$ s (f) $t = 118$ s

Figure 12: Snapshots of experimental data at different instants of time during execution. Red and blue circles represent the buoys to be separated, the triangles are the ASVs and the stars are their initial positions. Dashed curves are the planned trajectories. Solid curves are the (post-processed) shape of the cable as obtained from the camera data. Mild drifting of the objects (due to tugging by the cable) during experiment can be observed. Deviation of the actual paths followed by the ASVs from the planned paths (dotted curves) was due to the inability of the underactuated ASVs to compensate for the large drag on the floating cable. Also see Extension 1.

6 Conclusions

In this paper we present a formal mathematical description of the problem of planning and control for a flexible cable towed by two robots so as to separate two types of objects in a planar environment. We develop a graph search-based implementation, and distribute the computation for efficiency. We demonstrate the working of the algorithms through simulations, and the practical applicability of the method using a dynamic simulation and experiments with ASVs. More elaborate experimentation with ASVs is within the scope of future research.

Acknowledgements

We gratefully acknowledge the support of the Office of Naval Research grant numbers N00014-07-1-0829 and N00014-09-1-1031, the Army Research Laboratory grant number W911NF-10-2-0016 and the Air Force Office of Scientific Research grant number FA9550-10-1-0567. We would also like to thank the reviewers, whose valuable comments and suggestions helped in vastly improving the quality of the paper.

Appendix

A. Index to Multimedia Extensions

Extension	Media Type	Description
1	Video	Dynamic simulations and field experiment.

B. Words as Homotopy Invariants – Generalization and Justification

For a pointed space, X, with basepoint x_0 (*i.e.* a space with a preferred point through which all closed curves pass), the construction of a *homotopy invariant* for closed curves can be formally (and with greater generality) justified using the van Kampen's theorem [Hatcher 01, Crowell 59] as follows:

Given a N-dimensional connected topological space, X (the *free* workspace), suppose we can find α counts of $(N-1)$-dimensional subsets, $U_1, U_2, \cdots, U_\alpha \subset X$ (the U_i's constitute the 'rays' in the earlier discussion – see Figure 13) such that:

i. $X_0 := X - \cup_{i=1}^{\alpha} U_i$ is simply-connected,

ii. $X_j := X - \bigcup_{i=1, i\neq j}^{\alpha} U_i$ are path-connected and $\pi_1(X_j) \simeq \mathbb{Z}$ for all $j = 1, 2, \cdots, \alpha$, and

iii. $U_i \cap U_j = \emptyset, \ \forall i \neq j$

[Note that all these conditions are satisfied by choosing the *rays* emanating from ζ_i as the U_i's, as in our previous discussion.]

Using these properties it is easy to see that $X_i \cap X_j = X_0, \ \forall i \neq j$, and thus the set $C = \{X_0, X_1, X_2, \cdots, X_\alpha\}$ constitutes an open over of X that is closed under intersection. These are essential requirements for the van Kampen's theorem (see Section 1.2 of [Hatcher 01]) to be applied on an open cover of X.

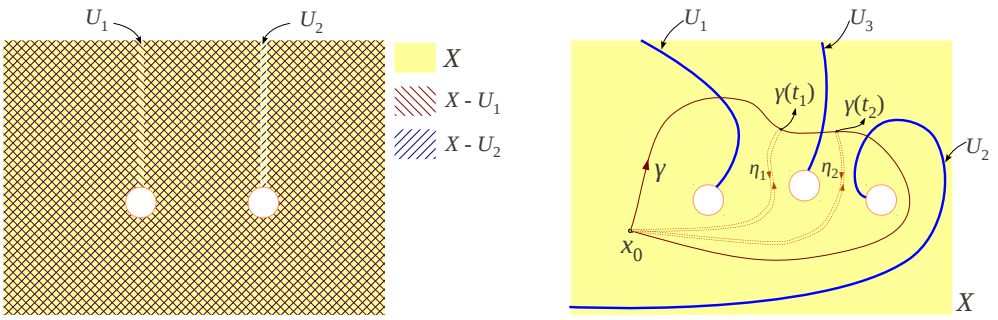

(a) The topological space X and its cover constituting of $X_i = X - U_i, \ i = 1, 2, \cdots$.

(b) U_i's different from 'rays'. The closed curve γ, and the division of the interval $[0, 1]$ is shown.

Figure 13: Use of van Kampen's theorem for justification of proposed homotopy invariants and its generalization.

Now it follows from the van Kampen's theorem that the first homotopy group of X is isomorphic to the (non-abelian) *free product* [Scott 64] of the first homotopy groups of $X_0, X_1, X_2, \cdots, X_\alpha$. Furthermore, note that $\pi_1(X_0) \simeq 0$ and $\pi_1(X_i) \simeq \mathbb{Z}, \ i = 1, 2, \cdots, \alpha$. Thus it is not a surprise

that homotopy classes in $\pi_1(X)$ can be expressed as "words" generated by α letters – one for each generator of a subgroup $\pi_1(X_i) \simeq \mathbb{Z}$. The more challenging part is to actually describe the map at the level of closed curves that induces the isomorphism of the homotopy groups. For that we borrow the construction appearing in proof of van Kampen's theorem (Theorem 1.20) of [Hatcher 01]:

Given a closed curve $\gamma : [0,1] \to X$, with $\gamma(0) = \gamma(1) = x_0$ (the base-point in X), we divide the interval $[0,1]$ as $0 = t_0 < t_1 < \cdots < t_m = 1$ such that $\gamma(t_k) \in X_0,\ \forall k$, and $\gamma([t_k, t_{k+1}])$ lies entirely in $X_{\iota(k)},\ \iota(k) \in \{1, 2, \cdots, \alpha\}$ (equivalently, $\gamma([t_k, t_{k+1}])$ intersects only with $U_{\iota(k)}$. This is always possible since we assume everything is Hausdorff). We can then construct curves, η_i such that $\eta_i(0) = \gamma(t_i)$ and $\eta_i(1) = x_0$, lying completely in X_0, as illustrated in Figure 13(b) (this is always possible since X_0 is path connected). Then clearly γ is homotopic to $\xi := \xi_0 \sqcup \xi_1 \sqcup \cdots \sqcup \xi_{m-1}$, where $\xi_0 := \gamma|_{[t_0,t_1]} \sqcup \eta_1,\ \xi_1 := -\eta_1 \sqcup \gamma|_{[t_1,t_2]} \sqcup \eta_2,\ \xi_2 := -\eta_2 \sqcup \gamma|_{[t_2,t_3]} \sqcup \eta_3,\ \cdots, \xi_k := -\eta_k \sqcup \gamma|_{[t_k,t_{k+1}]} \sqcup \eta_{k+1}, \cdots,\ \xi_{m-1} := -\eta_{m-1} \sqcup \gamma|_{[t_{m-1},t_m]}$. It is easy to observe that each ξ_k is a closed curve that lies completely inside $X_{\iota(k)}$, and since $\pi(X_{\iota(k)}) \simeq H_1(X_{\iota(k)}; \mathbb{Z}) \simeq \mathbb{Z}$ (the first isomorphism holds due to Hurewicz theorem [Hatcher 01]), the homotopy and homology invariants of closed curves in $X_{\iota(k)}$ are the same. Thus $[\xi_k] \in \pi(X_{\iota(k)})$ is represented by the winding number of ξ_{k+1}, which in turn is computed by the *intersection number* [Dold 95, Bhattacharya 13] between ξ_k and $U_{\iota(k)}$ (which is equal to the 'intersection number' between $\gamma([t_k, t_{k+1}])$ and $U_{\iota(k)}$, since the η_*'s do not intersect any of the U_*'s).

Thus in conclusion, the homotopy class of γ is represented as $[\gamma] = [\xi] = [\xi_0] \star [\xi_1] \star \cdots \star [\xi_{m-1}]$, where '$\star$' indicates the free product, and the elements $[\xi_k] \in \pi(X_{\iota(k)}) \simeq H_1(X_{\iota(k)}; \mathbb{Z}) \simeq \mathbb{Z}$ are represented as unique 'letters' exponentiated by the intersection number between ξ_k and $U_{\iota(k)}$.

It is to be noted that the choice of the subsets U_i such that the mentioned conditions are satisfied is not unique. This indeed hints towards the equivalence of the different representations of homotopy invariants as *words* that are found in literature [Grigoriev 98, Hershberger 91, Tovar 08, Hatcher 01, Bhattacharya 12a, Narayanan 13].

References

[Aranda 06] Joaqun Aranda, Pablo Gonzlez de Santos & Jess Manuel de la Cruz. Robotics and automation in the maritime industries. Produccin Grfica Multimedia (PGM), 2006.

[Bhattacharya 10] Subhrajit Bhattacharya, Vijay Kumar & Maxim Likhachev. *Distributed Optimization with Pairwise Constraints and its Application to Multi-robot Path Planning*. In Proceedings of Robotics: Science and Systems, Zaragoza, Spain, 27-30 June 2010.

[Bhattacharya 11] Subhrajit Bhattacharya, Hordur Heidarsson, Gaurav S. Sukhatme & Vijay Kumar. *Cooperative Control of Autonomous Surface Vehicles for Oil Skimming and Cleanup*. In Proceedings of IEEE International Conference on Robotics and Automation (ICRA), 9-13 May 2011.

[Bhattacharya 12a] Subhrajit Bhattacharya. *Topological and Geometric Techniques in Graph-Search Based Robot Planning*. PhD thesis, University of Pennsylvania, January 2012.

[Bhattacharya 12b] Subhrajit Bhattacharya, Maxim Likhachev & Vijay Kumar. *Topological Constraints in Search-based Robot Path Planning*. Autonomous Robots, pages 1–18, June 2012. DOI: 10.1007/s10514-012-9304-1.

[Bhattacharya 13] Subhrajit Bhattacharya, David Lipsky, Robert Ghrist & Vijay Kumar. *Invariants for Homology Classes with Application to Optimal Search and Planning Problem in Robotics*. Annals of Mathematics and Artificial Intelligence (AMAI), vol. 67, no. 3-4, pages 251–281, March 2013. DOI: 10.1007/s10472-013-9357-7.

[Binder 81] D.A. Binder. *Approximations to Bayesian clustering rules*. Biometrika, vol. 68, pages 275–285, 1981.

[Bott 82] R. Bott & L.W. Tu. Differential forms in algebraic topology. Graduate texts in mathematics. Springer-Verlag, 1982.

[Catto 11] Erin Catto. *Box2D – A 2D Physics Engine for Games*, 2011. Available at http://box2d.org/.

[Cheng 09] P. Cheng, J. Fink & V. Kumar. *Cooperative Towing with Multiple Robots*. ASME Transactions: Journal of Mechanisms and Robotics, vol. 1, February 2009.

[Cormen 01] T. H. Cormen, C. E. Leiserson, R. L. Rivest & C. Stein. Introduction to algorithms. MIT Press, 2nd edition, 2001.

[Crowell 59] Richard H. Crowell. *On the van Kampen theorem*. Pacific J. Math., vol. 9, no. 1, pages 43–50, 1959.

[Derenick 13] Jason Derenick, Alberto Speranzon & Robert Ghrist. *Homological sensing for mobile robot localization*. In Robotics and Automation (ICRA), 2013 IEEE International Conference on, pages 572–579. IEEE, 2013.

[Dijkstra 59] Edsger W. Dijkstra. *A note on two problems in connexion with graphs*. Numerische Mathematik, vol. 1, pages 269–271, 1959.

[Dogar 12] Mehmet Dogar, Kaijen Hsiao, Matei Ciocarlie & Siddhartha Srinivasa. *Physics-Based Grasp Planning Through Clutter*. In Robotics: Science and Systems VIII, July 2012.

[Dold 95] A. Dold. Lectures on algebraic topology. Classics in mathematics. Springer, 2nd edition, 1995.

[Donald 00] Bruce Donald, Larry Gariepy & Daniela Rus. *Distributed Manipulation of Multiple Objects using Ropes*. In In IEEE International Conference on Robotics and Automation, pages 450–457, 2000.

[Fink 08] Jonathan Fink, M. Ani Hsieh & Vijay Kumar. *Multi-Robot Manipulation via Caging in Environments with Obstacles*. In IEEE International Conference on Robotics and Automation (ICRA), Pasedena, CA, May 2008.

[Gamelin 01] Theodore W. Gamelin. Complex analysis. Springer Science, 2001.

[Grigoriev 98] D. Grigoriev & A. Slissenko. *Polytime algorithm for the shortest path in a homotopy class amidst semi-algebraic obstacles in the plane*. In ISSAC '98: Proceedings of the 1998 international symposium on Symbolic and algebraic computation, pages 17–24, New York, NY, USA, 1998. ACM.

[Hart 68] P. E. Hart, N. J. Nilsson & B. Raphael. *A formal basis for the heuristic determination of minimum cost paths*. IEEE Transactions on Systems, Science, and Cybernetics, vol. SSC-4, no. 2, pages 100–107, 1968.

[Hatcher 01] Allen Hatcher. Algebraic topology. Cambridge Univ. Press, 2001.

[Hershberger 91] J. Hershberger & J. Snoeyink. *Computing Minimum Length Paths of a Given Homotopy Class*. Comput. Geom. Theory Appl, vol. 4, pages 331–342, 1991.

[Ivan 13] V. Ivan, D. Zarubin, M. Toussaint, T. Komura & S. Vijayakumar. *Topology-based Representations for Motion Planning and Generalisation in Dynamic Environments with Interactions*. International Journal of Robotics Research (IJRR), vol. 32, no. 9-10, pages 1151–1163, 2013.

[Jiang 10] Qimi Jiang & Vijay Kumar. *The Inverse Kinematics of 3-D Towing*. Advances in Robot Kinematics: Motion in Man and Machine, pages 321–328, 2010.

[Kerr 10] Richard A. Kerr. *A Lot of Oil on the Loose, Not So Much to Be Found*. Science, vol. 329, no. 734, 2010.

[Kim 13] Soonkyum Kim, Subhrajit Bhattacharya & Vijay Kumar. *Dynamic Simulation of Autonomous Boats for Cooperative Skimming and Cleanup*. Rapport technique, Portland, USA, August 4-7 2013.

[Kuderer 13] Markus Kuderer, Henrik Kretzschmar & Wolfram Burgard. *Teaching Mobile Robots to Navigate in Populated Environments*. In Proceedings of the International Conference on Intelligent Robots and Systems (IROS), Tokyo, Japan, 2013.

[Lamiraux 01] F. Lamiraux & L. E. Kavraki. *Planning Paths for Elastic Objects under Manipulation Constraints*. International Journal of Robotics Research, vol. 20, no. 3, pages 188–208, 2001.

[Munkres 99] James Munkres. Topology. Prentice Hall, 1999.

[Narayanan 13] Venkatraman Narayanan, Paul Vernaza, Maxim Likhachev & Steven M LaValle. *Planning under topological constraints using beam-graphs*. In Robotics and Automation (ICRA), 2013 IEEE International Conference on, pages 431–437. IEEE, 2013.

[Robertson 10] Campbell Robertson & Clifford Krauss. *Gulf Spill Is the Largest of Its Kind, Scientists Say*. The New York Times, August 2010.

[Saha 06] Mitul Saha, Pekka Isto & Jean claude Latombe. *Motion planning for robotic manipulation of deformable linear objects*. In in Proc. IEEE Int. Conf. Robot. Autom, pages 2478–2484, 2006.

[Samar 07] Sikandar Samar, Stephen Boyd & Dimitry Gorinevsky. *Distributed Estimation via Dual Decomposition*. 2007.

[Scott 64] W.R. Scott & W.R. Scott. Group theory. Dover Books on Mathematics Series. Dover Publ., 1964.

[Stanley 00] R.P. Stanley & G.C. Rota. Enumerative combinatorics:. Cambridge studies in advanced mathematics. Cambridge University Press, 2000.

[Suykens 99] J. A. K. Suykens & J. P. L. Vandewalle. *Least squares support vector machine classifiers*. Neural Processing Letters, vol. 9, no. 3, pages 293–300, Jun 1999.

[Tovar 08] Benjamn Tovar, Fred Cohen & Steven M. LaValle. *Sensor Beams, Obstacles, and Possible Paths*. In Workshop on the Algorithmic Foundations of Robotics, pages 317–332, 2008.